Global Change Biology
celebrating 20 years

Global Change Biology (2014) **20**, 1251–1263, doi: 10.1111/gcb.12364

Modeling daily flowering probabilities: expected impact of climate change on Japanese cherry phenology

JENICA M. ALLEN*, MARIA A. TERRES†, TOSHIO KATSUKI‡, KOJIRO IWAMOTO§, HIROMI KOBORI¶, HIROYOSHI HIGUCHI‖, RICHARD B. PRIMACK**, ADAM M. WILSON††, ALAN GELFAND† and JOHN A. SILANDER JR*

*Department of Ecology and Evolutionary Biology, University of Connecticut, 75 North Eagleville Road Unit 3043, Storrs CT 06269-3043, USA, †Department of Statistical Science, Duke University, Box 90251, Durham NC, 27708-0251, USA, ‡Forest Bio-Research Center, Forestry and Forest Products Research Institute, 1 Matsunosato, Tsukuba Ibaraki 305-8687, Japan, §Tama Forest Science Garden, Forestry and Forest Products Research Institute, 1833-81 Todori, Hachioji, Tokyo 193-0843, Japan, ¶Department of Environmental and Information Studies, Tokyo City University, 3-3-1 Ushikubo-nishi, Tsuzuki-ku, Yokohama 224-0015, Japan, ‖Graduate School of Media and Governance, Keio University, SFC Fujisawa, Kanagawa 252-0882, Japan, **Biology Department, Boston University, 5 Cummington Street, Boston, MA 02215, USA, ††Department of Ecology and Evolutionary Biology, Yale University, 165 Prospect Street, New Haven, CT 06520, USA

Abstract

Understanding the drivers of phenological events is vital for forecasting species' responses to climate change. We developed flexible Bayesian survival regression models to assess a 29-year, individual-level time series of flowering phenology from four taxa of Japanese cherry trees (*Prunus spachiana*, *Prunus* × *yedoensis*, *Prunus jamasakura*, and *Prunus lannesiana)*, from the Tama Forest Cherry Preservation Garden in Hachioji, Japan. Our modeling framework used time-varying (chill and heat units) and time-invariant (slope, aspect, and elevation) factors. We found limited differences among taxa in sensitivity to chill, but earlier flowering taxa, such as *P. spachiana*, were more sensitive to heat than later flowering taxa, such as *P. lannesiana*. Using an ensemble of three downscaled regional climate models under the A1B emissions scenario, we projected shifts in flowering timing by 2100. Projections suggest that each taxa will flower about 30 days earlier on average by 2100 with 2–6 days greater uncertainty around the species mean flowering date. Dramatic shifts in the flowering times of cherry trees may have implications for economically important cultural festivals in Japan and East Asia. The survival models used here provide a mechanistic modeling approach and are broadly applicable to any time-to-event phenological data, such as plant leafing, bird arrival time, and insect emergence. The ability to explicitly quantify uncertainty, examine phenological responses on a fine time scale, and incorporate conditions leading up to an event may provide future insight into phenologically driven changes in carbon balance and ecological mismatches of plants and pollinators in natural populations and horticultural crops.

Keywords: Bayesian, *Prunus jamasakura*, *Prunus lannesiana*, *Prunus spachiana*, *Prunus* × *yedoensis*, survival model, time to event model, vernalization, weather

Received 13 December 2012; revised version received 16 July 2013 and accepted 5 August 2013

Introduction

Phenological events are indicators of the biological response to climate change. Global meta-analyses have demonstrated that organisms are shifting their activity periods in response to changes in climate (Parmesan & Yohe, 2003; Root *et al*., 2005; Menzel *et al*., 2006; Primack *et al*., 2009). In the context of climate change, we seek to identify the drivers of phenological events so that we can make predictions about how individual species may respond and how certain we are about those predictions. We apply statistical tools not previously used in plant phenology with a mechanistic underpinning to improve forecasting ability and to explicitly quantify uncertainty in those forecasts.

The physiological mechanisms controlling bud burst and flowering are not precisely known, but it is clear that the timescale of response is temporally much finer than a monthly average can provide (Arora *et al*., 2003; Schaber & Badeck, 2003; Jimenez *et al*., 2010). Temperate deciduous plants often have chilling requirements, such that they must experience a period of cold temperature before warmer temperatures can trigger bud break and flowering events in spring (Hanninen, 1990; Kramer, 1994; Chuine, 2000; Menzel *et al*., 2006; Luedeling *et al*., 2009a; Jimenez *et al*., 2010; Polgar & Primack, 2011). Chilling and heating requirements may also trade-off, such that higher or longer duration warm temperatures are needed when cold temperatures are

Correspondence: Jenica M. Allen, tel. +1 860 486 8964, fax +1 860 486 6364, e-mail: jenica.allen@uconn.edu

suboptimal (Cannell & Smith, 1984, 1986; Caffarra *et al*., 2011). It is common to assume that plants always reach their chilling requirements in the temperate zone, but this may not be the case under climate change scenarios (Yua *et al*., 2010; Cook *et al*., 2012).

Temperature accumulation models incorporate physiological processes in phenology. The timing of phenological events (e.g., bud break, growth, flowering) is regulated primarily by temperature in the spring (Jimenez *et al*., 2010) and triggered by the accrual of sufficient chilling and heating (Thompson & Clark, 2006; Jimenez *et al*., 2010). Measured temperatures are typically converted to chill and/or heat units using one of a variety of algorithms, each of which represents a different assumption of how temperature drives plant physiology toward bud break (Chuine, 2000; Luedeling *et al*., 2009a). Accumulation models must also define the ways in which chilling and heating processes interact. In the simplest model, chill is ignored and only heat accumulates (Linkosalo *et al*., 2006). However, many temperate woody species, including cherries, require both chilling and heating (Hanninen, 1990; Kramer, 1994; Chuine, 2000; Menzel *et al*., 2006; Luedeling *et al*., 2009a; Jimenez *et al*., 2010; Polgar & Primack, 2011). Chill and heat units may accumulate in *parallel*, where both are affecting potentially different physiological processes simultaneously, *partially parallel,* where chilling and heating processes overlap for a shorter period of time, or *sequentially*, where chill units accumulate to a threshold followed by heat accumulation after the chill requirement is met (Hanninen, 1990; Kramer, 1994; Chuine, 2000). Which of these chill/heat relationships represents reality, and whether that reality varies among species, is unclear.

Accumulation models can estimate springtime phenology, but as typically implemented they do not fully quantify the uncertainty in model predictions or parameter estimates. To meet this challenge, we applied Bayesian survival regression models to incorporate the strengths of both linear regression and mechanistically based accumulation models (Venables & Ripley, 2002). In general, survival models are a class of methods that provide a way to analyze time-to-event data (i.e., a series of binary event occurrence observations through time). These models are used extensively in the medical field to predict how various treatments affect the survival of patients over time. In our case, the event of interest is tree flowering rather than patient survival. Daily survival models are similar to accumulation models in that they can incorporate short-term weather events that may impact the cumulative flowering probability and do not require aggregating antecedent weather conditions (thus avoiding the Modifiable Temporal Unit Problem, de Jong & de Bruin, 2012). Our approach fits with growing recognition that daily weather should be used to assess plant phenology (Pau *et al*., 2011) and can quantify uncertainty, an important aspect of climate change studies. To our knowledge, very few studies have applied survival analysis to phenological data, and none to plants (Gienapp *et al*., 2005; van de Pol & Cockburn, 2011; Visser *et al*., 2011).

In contrast to the few previous studies, which have used Proportional Hazards survival models (Gienapp *et al*., 2005; Martinussen & Scheike, 2006; van de Pol & Cockburn, 2011; Visser *et al*., 2011), we have employed a flexible, discrete-time, semi-parametric Bayesian survival model (Wilson *et al*., 2010; Terres *et al*., 2013). By fitting the model in a Bayesian framework, we are able to fully quantify uncertainty for estimated parameters and obtain full probability distributions for the predicted phenological event (Clark, 2004; Ellison, 2004). The full probability distribution can reveal patterns, such as asymmetries in the credible intervals around the predicted date, which would otherwise be hidden. The general modeling framework we use can be translated to other systems or sites to investigate any phenophase.

Cherry flowering data from the Tama Forest Cherry Preservation Garden (Hachioji, Japan) provide a well-replicated time series with associated environmental data and climate change projections. Previous linear regression analysis of this data set used monthly average springtime temperatures and showed consistent ordering of taxa and individuals within taxa in their flowering time and higher responsiveness to temperature in early flowering taxa relative to later flowering taxa (Miller-Rushing *et al*., 2007). In this traditional approach, no attempt was made to determine the effect of chilling. The goals of this study were to employ daily-resolution Bayesian survival regressions that incorporated both heating and chilling to understand the drivers of historical phenology and predict future flowering dates for a suite of cherry taxa. We expected both chill and heat to be important drivers of current flowering phenology. In addition, we anticipated accelerated future flowering if chill requirements could still be met under projected future climate, but delays if chilling requirements were no longer met.

Materials and methods

Flowering & microsite data

First flowering observations were obtained from the Tama Forest Cherry Preservation Garden (35.6490°N, 139.2749°E, 8 ha), located just outside Hachioji, Japan for the years 1981–2009 (Fig. 1). The cherry flowering data set comprised 17 species

and hybrids in the genus *Prunus*. We used the four most replicated taxa, *Prunus spachiana* ($n = 4$), *Prunus* × *yedoensis* ($n = 14$), *Prunus jamasakura* ($n = 10$), and *Prunus lannesiana* ($n = 42$) in our analysis, which included the focal species of many cherry blossom festivals (the Yoshino cherry, *P.* × *yedoensis*). First flowering observations, defined as 2–3 open flowers on the tree, were made every 2–3 days in early spring and estimated on a daily timescale as described in Nagata and Yurigi (1982). Mean first flowering date for each species was consistently ordered year after year, with *P. spachiana* flowering first, followed in order by *P.* × *yedoensis*, *P. jamasakura*, and *P. lannesiana* and individual trees within a species were ordered similarly (though not exactly) year after year. There was overlap in flowering time among the latest trees of the early species and the earliest trees of the otherwise later species.

Aspect, slope, and elevation were measured for each individual tree. The site is topographically heterogeneous, so we expected topographic features to serve as proxies for spatial effects among tree locations. Microsite factors may represent microclimate, edaphic factors such as hilltop vs. valley bottom soils or soil moisture, or biotic effects such as spatial variation in trophic interactions (Gonzalez-Megıas & Menendez, 2012) or in soil microbes and concomitant nutrient availability (Nord & Lynch, 2009). Slope and aspect were combined into east-westness [EW = sin(slope*π/180)*sin(aspect*π/180)] and north-southness [NS = sin(slope*π/180)*cos(aspect*π/180)] indices, which more accurately reflect the combined influence of the input variables on the amount of solar radiation a tree receives in addition to soil moisture variation, cold air drainage, etc. (Sherman *et al*., 2008). Each index varies from −1 to 1, with a value of −1 indicating a due western or northern aspect and 90° slope and a value of 1 indicating a due eastern or southern aspect with 90° slope, for EW and NS, respectively. These metrics tend toward 0 as slope decreases and equals 0 where the slope is 0.

Historical weather data

Hourly temperature and sunlight hours from the Japanese Meteorological Agency Hachioji AMeDAS Station (Automated Meteorological Data Acquisition System), located 4 km from the Tama Forest Garden, were used to calculate chill, heat, and sunlight hours metrics. Sunlight hours measure the amount of 'bright' sunlight (that over 120 W m^{-2}) relative to a clear day in a given period of time (expressed as a proportion) and are positively correlated to solar radiation received at the Earth's surface (Suehrcke *et al*., 2013). Low proportion to no sunlight hours may be recorded between sunrise and sunset under cloudy conditions (Suehrcke *et al*., 2013). Multiple chill unit formulations exist to weight hourly temperatures based on their effects on plant physiological responses (Luedeling *et al*., 2009a). We chose two chill unit formulations based on hourly temperature data: Chill Hours (CH) and Utah Units (UT). Chill Hours are calculated using a threshold function and take values of 0 or 1 (Table 1). Utah Units are calculated using a step function that includes a penalty for exceptionally high temperatures and range from −1 to 1 (Table 1). Heat Units were defined by the Growing Degree Hour model (Luedeling *et al*., 2009a) and range from 0 to 21. For chill and heat units, threshold and baseline temperatures were derived from studies of flowering fruit trees, one of which focused on cherries (Richardson *et al*., 1974; Alburquerque *et al*., 2008; Luedeling *et al*., 2009a) and were calculated using hourly data then summed to daily.

We explored two chill/heat relationships, parallel and sequential, and daily contribution vs. cumulative weather models. We created a 'daily contribution' data set by calculating chill and heat units for each day's observed temperature, but we did not accumulate chill or heat across days. To create a 'cumulative weather' data set, we calculated each day's chill and heat units based on observed temperature, and then accumulated those values according to both parallel and sequential

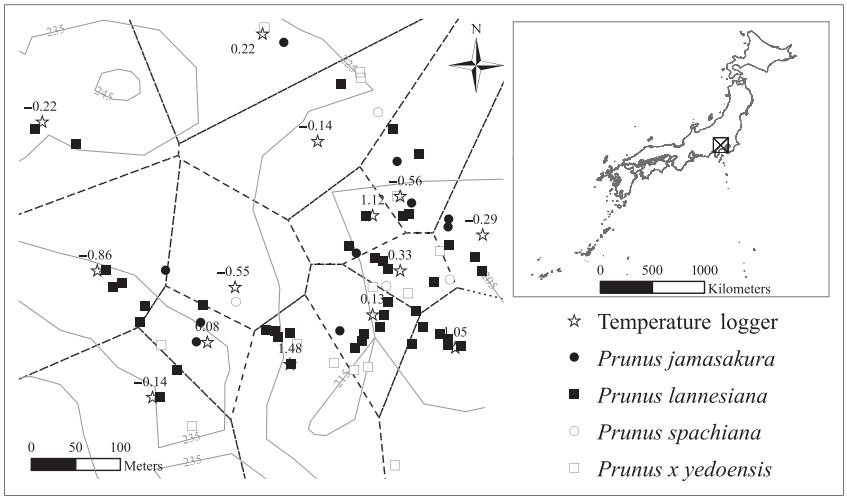

Fig. 1 The Tama Forest Cherry Preservation Garden in Hachioji, Japan. Points indicate individual tree locations (each taxon coded by shape and color) and temperature logger locations within the site. Average daily temperature anomalies (°C) between the Hachioji Meteorological Station and each temperature logger for July 2009 to May 2010 are labeled for each logger. Trees within each dashed line polygon are assigned the anomaly from the HOBO logger within that polygon. Elevation contours are provided in meters and the inset indicates the location of Hachioji in Japan.

Table 1 Conversion of observed hourly temperature (T) to chill units using the Chill Hour and Utah Unit algorithms

	Temperature	Chill units
Chill Hours (CH)	T<0 °C	0
	0 °C ≤ T ≤7.2 °C	1
	T > 7.2 °C	0
Utah Units (UT)	$T \leq 1.4°$	0
	1.4 °C < T ≤ 2.4 °C	0.5
	2.4 °C < T ≤ 9.1 °C	1
	9.1 °C < T ≤ 12.4 °C	0.5
	12.4 °C < T ≤ 15.9 °C	0
	15.9 °C < T ≤ 18 °C	−0.5
	T > 18°	−1

accumulation models. The cumulative weather data set reflects the common construction of accumulation models. We included the daily contribution comparison to confirm the need for accumulated weather metrics in conjunction with a time-series model, despite our expectation that cumulative weather metrics would reflect known biological mechanisms. For the parallel model, we calculated the cumulative sum of daily chill and heat units from January 1 of each year. In this case, heat and chill units accumulated simultaneously, with chill accumulating rapidly early in the year and heat accumulating rapidly later in the spring (due to the optimal thresholds in the chill and heat unit formulations, Table 1). The sequential model required that we set a chill requirement value to trigger the switch from chill accumulation to heat accumulation. Non-identifiability precluded fitting the chill requirement as a model parameter (a common problem in statistical modeling, cf. Dasguptaa *et al*., 2007), so we used a cumulative Utah Unit threshold of 754 units based on the mean chilling requirement of *Prunus avium* (sweet cherry) cultivars determined from laboratory study (Alburquerque *et al*., 2008). We accumulated chill only until the date that the Utah Unit chill threshold was reached each year and accumulated heat only after the chill threshold had been met. Our January 1 chill accumulation start date for both chill/heat relationships is in accordance with current knowledge of genetic controls on phenology. In the species studied thus far, a cluster of several 'Dormancy Associated MADS-box transcription factors' genes are up-regulated by decreasing day-length resulting in the onset of plant dormancy in the fall (Jimenez *et al*., 2010). The up-regulation of these dormancy genes reaches a peak at winter solstice, after which chilling temperatures act antagonistically to promote plant development (Jimenez *et al*., 2010). All calculations of daily chill and heat units (and cumulative values) were completed external to and served as the input covariate matrix for statistical models.

We expected the microsite factors to serves as proxies for differences in site-level environmental conditions. We installed HOBO temperature loggers (Onset Corp., Pocasset, MA, USA) at the Tama Forest Garden in July 2009 to investigate local temperature variation as an alternative to our suite of site-level spatial factors (slope, aspect, elevation). Fifteen loggers were dispersed around the property in areas chosen to maximize the variance in microsite characteristics (Fig. 1). Each logger was attached to a tree trunk (not necessarily one of the trees in our data set) about 1.5 m from the ground and oriented to use natural shading (e.g., under a limb). Mean temperature was recorded every 2 h from late July 2009 to early May 2010. These data were summarized to daily mean temperatures and compared directly to daily mean temperatures from the Hachioji Meteorological Station. We calculated daily-scale temperature anomalies as the station mean daily temperature minus HOBO mean daily temperature and subsequently averaged across the period of record to create an average temperature anomaly per logger location. The temperature anomaly of the closest HOBO logger was assigned to each individual tree in the data set (Fig. 1).

Projected weather data

Statistically downscaled climate model projections for the Hachioji Meteorological Station were obtained from the ELPIS-JP data set (Iizumi *et al*., 2012). We used the regional climate model (RCM) ensemble that included the NHRCM, NRAMS, and TWRF models, all driven by the MIROC-H GCM under the A1B scenario (Iizumi *et al*., 2012). In order to assess the shifts in first flowering dates under climate change scenarios, we used both historical (1981–2000) and future (2081–2100) daily temperature data. ELPIS-JP data were provided as a 20-year average of daily mean temperature for each period (historic and future) for each model (Iizumi *et al*., 2012). In other words, we had one value for each day of year that represented an average of 20 years of simulation (1981–2000, 2081–2100). We used model output temperature values instead of the station data for the historical prediction in addition to future forecasts in this comparison to account for any possible climate model bias.

For future weather RCM scenarios, hourly temperature data are not available, so we rescaled the UT threshold to match daily calculations. To accomplish this rescaling, we calculated UT chill and heat units for the historical station data after aggregating it to daily mean temperature. We then matched the day of year when the hourly based chill requirement was met to this daily-derived data set. The range of daily-derived UT threshold values ranged from 28.5 to 50, and we took the average to establish the rescaled chill threshold (42 Utah chill units).

Statistical analysis

The analysis of first flower dates was performed using a discrete time semi-parametric survival model, estimating the probability that a tree 'fails to flower' on each day of a given year. Our model specifies an explicit regression equation incorporating time varying covariates (i.e., chill and/or heat) for each individual to explain the phenological observation. The basic structure is similar to a time-to-fire model previously developed for the Cape Floristic Region of South Africa (Wilson *et al*., 2010), but is modified for less complex data (Terres *et al*., 2013).

The model is run for each taxon individually and uses the binary daily (t) phenology observations (1 indicating the date of budburst) from each individual tree (i) in every year (y) beginning January 1. The first flowering date for individual i in year y, where the date is considered to be the number of days since the beginning of chill accumulation, is denoted Z_{iy}. For each day, we model the probability of not flowering on that day given that flowering has not yet occurred, denoted $p_{iyt} = P(Z_{iy} > t \mid Z_{iy} > t-1)$. The concept of a survival function, $S_{iy}(t)$, is common in survival analysis and in our case corresponds to the probability that the individual tree flowers sometime later than day t. Here, the survival function on day t for individual i in year y is equal to the product of non-flowering probabilities of that day t and all preceding days in that year y, or $S_{iy}(t) = P(Z_{iy} > t) = p_{iyt}p_{iy,t-1} \cdot \cdot \cdot p_{iy1}$, such that the entire time series of flowering probabilities (a function of the covariates) for individual i up to day t is taken into account. The models are fit for each taxon treating each individual as an independent replicate, such that we can compute a taxon level survival function $S(t)$ for each year in the data set. From the survival function $S(t)$, we can then compute the unconditional probability of flowering on each day (we term this 'daily flowering probability') by taking the difference of cumulative flowering probability up to day t and the cumulative flowering probability up to the day prior ($t-1$), or $P(t-1 < Z_{iy} \leq t) = S(t-1) - S(t) = (1-p_{iyt})\ p_{iy,t-1} \cdot \cdot \cdot p_{iy1}$. Modeling p_{iyt} allows us to compute all of the probabilities of interest. To relate the environmental factors to the flowering probabilities, we used a probit link function: $\text{probit}(p_{iyt}) = X_{iyt}{}^T\beta$, where $X_{iyt}{}^T$ is a matrix of covariates (Tables 2 and 3) for each individual i in year y on day t. Normally distributed, non-informative priors [Normal(0,1000)] were used for all regression coefficients. Additional technical development is available in Terres *et al*. (2013).

Our candidate covariates (Table 2) and candidate models (Table 3) included combinations of chill units, heat units, sunlight hours, microsite factors (EW, NS, elevation), and temperature anomalies measured by HOBO loggers for 1 year (see details above). We tested two formulations of chill units (CH and UT), two chill/heat relationships (parallel and sequential), and models with daily chill and heat contributions vs. accumulated chill and heat (see above) to determine which of these choices fit our data best with our new model application. We included microsite factors as a proxy for small-scale spatial variation in environmental conditions (e.g., temperature, soils, biotic effects) and a comparison with temperature anomalies to investigate which best captured site-level variation in phenology. We also included a comparison of models that included cumulative heat from January 1 with the microsite factors with and without cumulative UT chill to explicitly determine the importance of chilling. We attempted to fit a sequential and parallel chill/heat model using accumulated

Table 2 Model covariates, descriptions, and units

Covariate	Description	Units
Cumulative heat	Heat units, calculated using a growing degree hour model, accumulated from January 1 to the first flowering date of each year.	Hours within specified temperature thresholds (see text for heat unit details)
Cumulative chill	Chill units, calculated using either the Chill Hours (CH) or Utah (UT) algorithm, accumulated from January 1 to the first flowering date of each year.	Hours below or within specified temperature thresholds (see Table 1 for CH and UT thresholds)
North-southness	A time-invariant metric that combines slope and aspect in the north-south axis. Abbreviated as NS.	No units
East-westness	A time-invariant metric that combines slope and aspect in the east-west axis. Abbreviated as EW.	No units
Anomaly	The average daily temperature difference between measurements at the nearby weather station and temperature loggers installed within the Tama Forest Garden for 2009–2010.	°C
Sunlight hours	Proportion of bright light (over 120 W m^{-2}) received at the Earth's surface relative to that received in clear skies.	Proportional hours
Heat	Heat units, calculated using a growing degree hour model, for each day in each year.	Hours within specified temperature thresholds (see text for heat unit details)
Chill	Chill units, calculated using either the Chill Hours (CH) or Utah (UT) model, for each day in each year.	Hours below or within specified temperature thresholds (see Table 1 for CH and UT thresholds)

Table 3 Candidate models for four taxa of flowering cherries in *Prunus*

Model number	Chill type	Model parameters	Chill/heat relationship
1	UT	Cumulative heat + cumulative chill + NS + EW + elevation	Sequential
2	UT	Cumulative heat + cumulative chill + NS + EW + elevation + sunlight hours	Sequential
3	UT	Cumulative heat + cumulative chill + sunlight hours	Sequential
4	UT	Cumulative heat + cumulative chill	Sequential
5	UT	Cumulative heat + cumulative chill + NS + EW + elevation	Parallel
6	UT	Cumulative heat + NS + EW + elevation	Parallel
7	UT	Cumulative heat + cumulative chill + anomaly	Parallel
8	UT	Cumulative heat + cumulative chill + sunlight hours	Parallel
9	UT	Cumulative heat + cumulative chill	Parallel
10	UT	Cumulative heat	Parallel
11	UT	Daily heat + daily chill	Parallel
12	CH	Daily heat + daily chill	Parallel
13	UT	Sunlight hours	Parallel

UT chill units, accumulated heat, microsite factors, and sunlight hours, but were unable to achieve convergence for the sunlight hours parameter. Our final set of candidate models was 13 per taxon (Table 3).

Models were fit using MCMC techniques custom coded in R (R 2.13.1, R Core Team, 2011) and are supplied in Supplement S2. We centered and normalized all covariates across the entire time series for all taxa to aid in model convergence and model comparison. We ran three chains with 300 000 iterations per chain for each model and used the plot, autocorr.plot, and gelman.plot functions in the R package 'coda' (Plummer *et al.*, 2006) to visually assess model convergence and autocorrelation. We ultimately used a burn-in of 70 000 and thinning interval of 75 for a posterior sample of 9201 iterations per model. Model run time was not insignificant; the most highly replicated taxa (*C. lannesiana*, 42 individuals) required up to 4 days to run. We used deviance information criterion (DIC) for model selection, where lower DIC values indicated better model fit and included a penalty for model complexity (Spiegelhalter *et al.*, 2002). We considered a ΔDIC less than 2 to be insignificant, 2–10 to be moderately improved, and >10 to be significantly (not in a *P*-value sense) improved fit following standard convention. We calculated DIC values and regression coefficients from the posterior of β after burn-in and thinning.

We calculated the daily first flowering probabilities as $S(t-1)-S(t)$, where $S(t)$ is the survival function for each taxon at time t. The output of the model is a distribution of probabilities over days, so we selected the date with the highest probability of flowering as our estimated first flowering date. In the models presented, the time-varying covariates are cumulative and show no contraindicated behavior, such as large probability values early in the time series, that suggests max $S(t-1)-S(t)$ will produce spurious early season predicted first flower dates. We computed 95% highest posterior density (HPD) credible intervals for each daily flowering probability $[S(t-1)-S(t)]$ curve to quantify uncertainty in our first flowering date estimates. In contrast to other techniques that would always produce a symmetric 95% interval centered at the estimate, a HPD credible interval finds the narrowest interval of days containing 95% of the probability mass, which may be asymmetric around the estimate (Gelman *et al.*, 2004). The 95% credible intervals around the daily flowering probabilities (see Fig. 5) suggest that the variability in the parameter estimates result in negligible uncertainty regarding the daily probability of flowering. Thus, when computing these HPD credible intervals, we use the mean probability distribution estimated by the model. Models were fit using the hourly derived chill and heat for model comparison and daily-derived weather data for forecasting based on future projection data availability.

We performed analysis on output from the three RCMs run under the A1B scenario. For each taxon, our model produced a probability distribution for first flowering date for each RCM. By treating each RCM as an equally likely projection for future weather, we averaged the summarized posterior samples of these three probability distributions to produce an estimated probability distribution for that taxon. HPD credible intervals were then computed using the projected probability distributions, producing 95% intervals for the ensemble first flowering dates of each taxon under the A1B scenario. These intervals do not directly incorporate the inherent uncertainty in the RCM models themselves, but by averaging across models we do account for uncertainty among RCMs. The difference in the temporal resolution of weather data acted to rescale the parameters so we could forecast using the available climate model projections.

Results

Models constructed with the Utah chill model had lower DIC values than models using the Chill Hours model for all four taxa (Model 11 vs. 12; Fig. 2). Models including sunlight hours lowered DIC values moderately for all taxa compared to models with only cumulative chill and heat, but much less than the addition of microsite factors to the model (Model 8 vs. 5; Fig. 2). Among the models using a parallel heat/chill relationship and Utah chill units, models based on cumulative

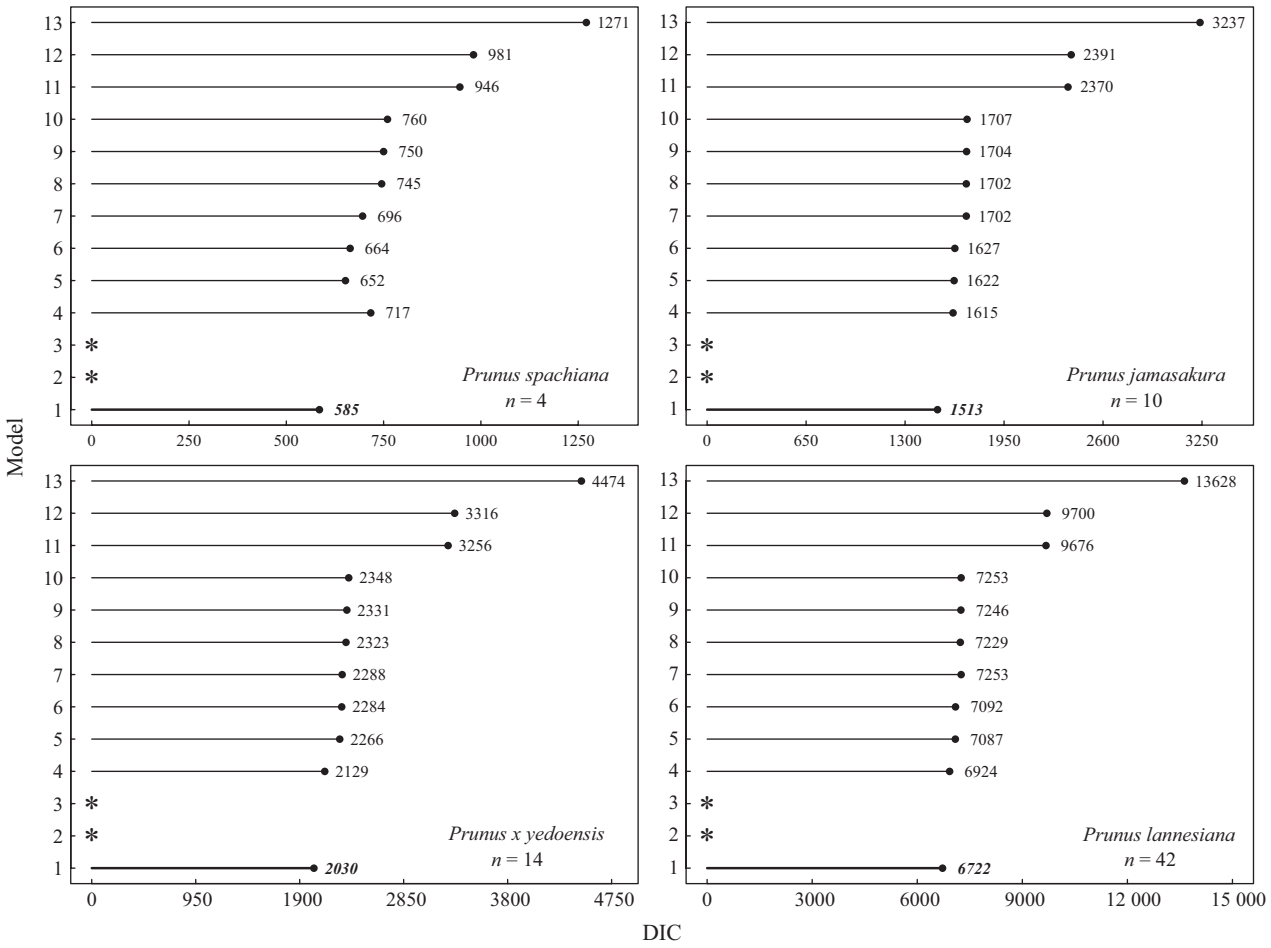

Fig. 2 Deviance Information Criterion (DIC) values for 13 candidate models (see Table 3) for *Prunus spachiana*, *Prunus jamasakura*, *Prunus* × *yedoensis*, and *Prunus lannesiana*. The best supported model (based on lowest DIC) for each taxon is indicated in bold italic. Asterisks (*) indicate that models did not converge.

chill and cumulative heat, rather than daily contributions of chill and heat, had lower DIC values indicating better support from the data (Model 11 vs. 9; Fig. 2). Models that included cumulative heat and chill fit better than models that included only cumulative heat (Model 9 vs. 10 and Model 5 vs. 6; Fig. 2). Parallel UT models that included the HOBO temperature anomalies had higher DIC values than models that included microsite factors instead (Model 7 vs. 5; Fig. 2). Finally, among models including parallel or sequential cumulative heat and cumulative chill based on Utah units, models including microsite factors (east-westness, north-southness, and elevation) fit the best for all species (Model 5 and 1; Fig. 2). For all subsequent analyses, we used the overall best fit model, which was the sequential model with cumulative heat, cumulative UT chill, and microsite factors (Model 1; Fig. 2).

We assessed the importance of each covariate in our best fit model by comparing standardized regression coefficients within and across species. In our modeling framework, negative coefficients correspond to an increased probability of flowering and positive coefficients correspond to a decreased the probability of flowering, with the magnitude of the effect reflected in the magnitude of the regression coefficient estimate. On average, the earliest flowering species, *P. spachiana*, had the greatest sensitivity to both chill and heat (i.e., largest coefficient), followed by *P.* × *yedoensis*, *P. jamasakura*, and *P. lannesiana* (Fig. 3). However, chill coefficient estimates overlapped zero for all taxa (Fig. 3). Coefficients for microsite factors were of smaller magnitude than those for temperature-derived metrics, but contributed significantly in all cases except NS and elevation for *P. spachiana* (Fig. 3).

The models presented here can estimate daily or cumulative probabilities of flowering. Predicted cumulative flowering probability curves varied in shape and location among years within a taxa based on

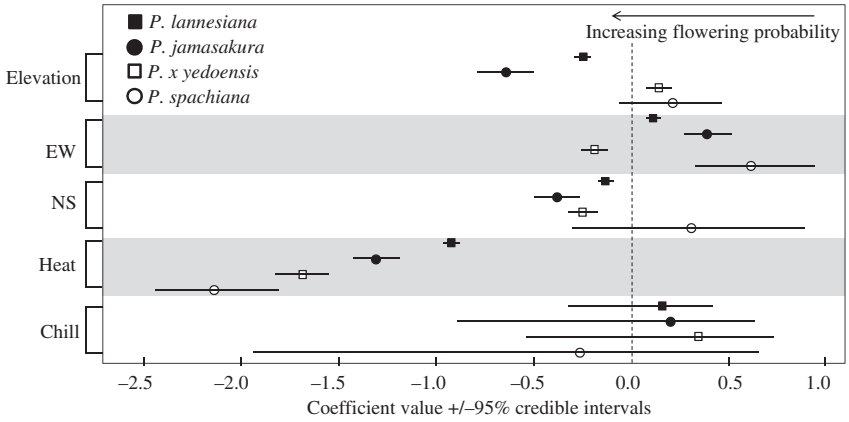

Fig. 3 Standardized regression coefficients for the best sequential model (Model 1). Negative coefficients mean the covariate promotes flowering and *vice versa*. Credible intervals that overlap zero are not statistically significant. Each taxon is coded by point shape and color.

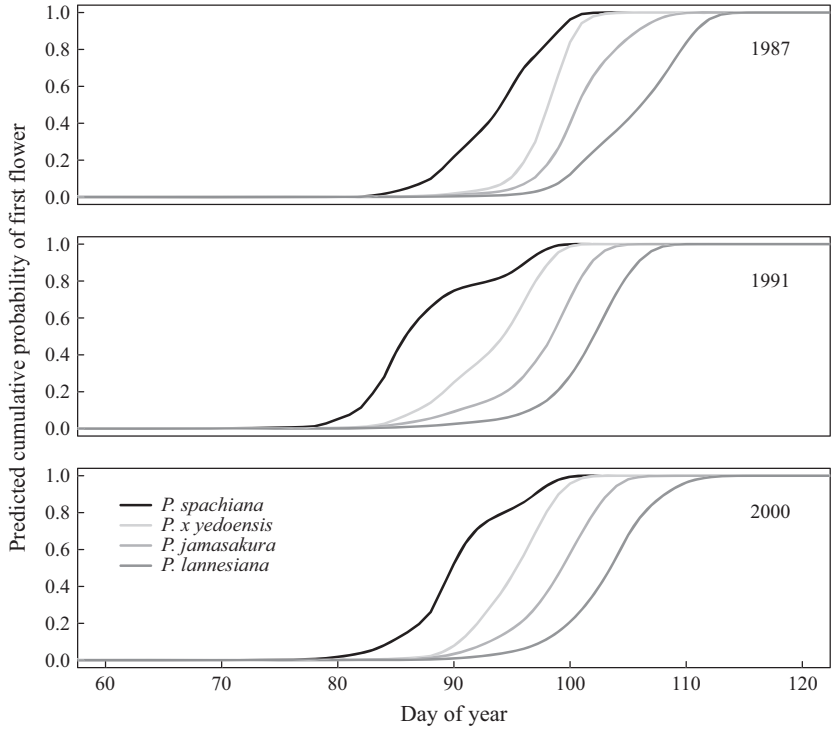

Fig. 4 Mean predicted cumulative first flowering probability, defined as $1-S_y(t) = 1-p_{yt}p_{y,t-1}\cdot\cdot\cdot p_{y1}$, for four cherry taxa in 3 years (1987, 1991, 2000) for the best sequential model (Model 1). Observed flowering order is preserved in model predictions and interannual variability is reflected in the shape of the curves. Each taxon is coded by color.

interannual weather variation (Fig. 4). Across taxa, the observed flowering order was replicated in the predicted cumulative flowering probability, such that the curves trended up and asymptoted in observed flowering order (*P. spachiana* < *P.* × *yedoensis* < *P. jamasakura* < *P. lannesiana*) (Fig. 4). The uncertainty around each mean estimate was greatest from about March to May each year (Figures S1, S3, S5, S7).

We used the day with the highest posterior flowering probability as the estimate of first flowering date. The best fit sequential model (Model 1) for each species provided tight estimates to observed first flower dates across years (Fig. 5; Figures S2, S4, S6, S8), with mean residuals of −0.4, 1.3, 1.3, and 1.6 days and root mean square errors of 4.02, 2.73, 2.78, and 3.13 days for *P. spachiana*, *P.* × *yedoensis*, *P. jamasakura*,

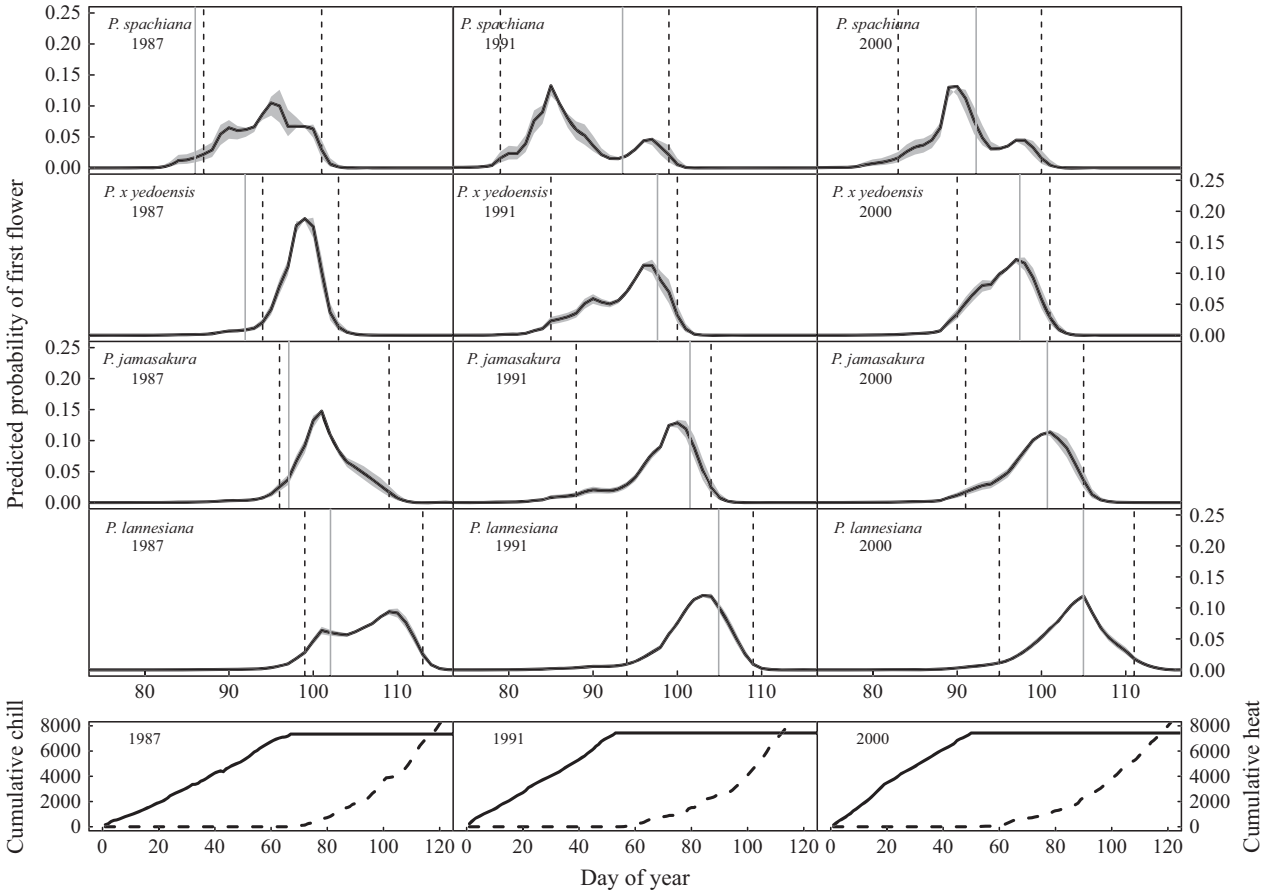

Fig. 5 Daily estimated probability of first flowering (solid black curve) and 95% credible intervals (gray shading) for four cherry taxa in 1987, 1991, and 2000, as defined by $S(t-1)-S(t)$. Annual observed taxon mean first flowering dates are indicated by solid gray vertical lines and the 95% highest posterior density (HPD) intervals of first flowering date predictions are indicated by dashed black vertical lines. The bottom row shows cumulative Utah chill (solid line) and heat (dashed line) units for the same years. These years represent two extremes of early and late flowering date predictions (1987, 1991) and an average year (2000) along with the associated temperature patterns at the site. Model predictions on average coincide well with observed first flowering dates (within 1–2 days), with slightly later predicted dates than observed in years with delayed fulfillment of chilling requirements (1987) and slightly earlier predicted dates than observed in years with early to average fulfillment of chilling requirements followed by faster than average heat accumulation (1991).

and *P. lannesiana*, respectively. The predicted and observed first flowering dates across species and years were very highly correlated, with Pearson correlation coefficients of 0.82, 0.92, 0.93, and 0.90 for *P. spachiana*, *P.* × *yedoensis*, *P. jamasakura*, and *P. lannesiana*, respectively. The largest differences between predicted and observed first flowering dates for most taxa were in 1987, when predictions were 4–9 days late. The weather in 1987 resulted in later than usual satisfaction of chilling requirements, due in part to a short-term temperature rise early in the season (Fig. 5; Figure S9). In 1991, heat accumulated more quickly than usual and yielded predictions that were earlier than observed (Fig. 5; Figure S9). In most years, however, chill requirements were met by late-February followed by progressively rapid heat accumulation, and these years yielded very tight predictions around observed values as indicated by the mean residuals and RMSE (Fig. 5; Figure S9; Table S1).

The Bayesian approach provided a full distribution for the flowering probabilities, allowing us to see how the shapes of these distributions vary across years and species. In some years, there was a peak in probability symmetrically spread across several days, while in other years there were multiple peaks slightly separated from one another (Fig. 5; Figures S2, S4, S6, S8). Multiple peaks suggest that there were two somewhat distinct periods of time during which flowering was likely to occur. Other statistical methods would not have allowed for the possibility of multiple peaks and would have assumed a symmetric spread of probabilities in all years for all species. Similarly, the Bayesian

approach allowed us to compute 95% HPD credible intervals. Considering the shape of our distributions, it was not surprising that these credible intervals were not symmetric around our first flowering date estimate, and as we would expect, almost all of our intervals encompassed the observed species mean first flowering date (Fig. 5; Figures S2, S4, S6, S8).

Future (2081–2100) mean temperatures at Hachioji are projected to be higher than the historical period (1981–2000) year-round. The springtime temperature rise will result in little change in sequential Utah chilling accumulation, but heat accumulation will be accelerated (Fig. 6). Under these conditions, we expect that on average, *P. spachiana*, *P. jamasakura*, and *P. lannesiana* will flower 30 days earlier and *P.* × *yedoensis* will flower 31 days earlier by 2100 under the A1B scenario (Fig. 7). The ensemble 95% HPD intervals for future flowering dates (as day of year) were (55, 77), (62, 80), (64, 85), and (67, 90) for *P. spachiana*, *P.* × *yedoensis*, *P. jamasakura*, and *P. lannesiana*, respectively. These future HPD intervals do not overlap the historical intervals for any taxa (Fig. 7); if flowering occurred at the earliest day of year within the historical HPD interval and the latest day in the future interval, we would still expect accelerated flowering of 7, 9, 12, and 8 days for *P. spachiana*, *P.* × *yedoensis*, *P. jamasakura*, and *P. lannesiana*, respectively. The ensemble 95% HPD interval for first flowering date estimates were 2, 5, 5, and 6 days wider in the future period relative to the historical period for *P. spachiana*, *P.* × *yedoensis*, *P. jamasakura*, and *P. lannesiana*, respectively, and showed a shift in asymmetry from greater uncertainty before the mean flowering estimate in the historical period to greater uncertainty after the estimate under future climate.

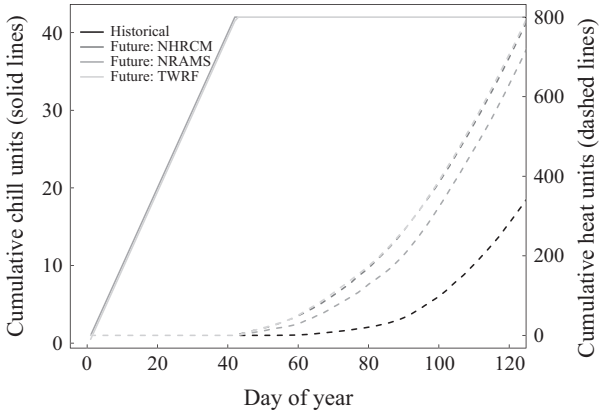

Fig. 6 Historical (1981–2000) and future (2081–2100) cumulative sequential Utah chill (solid lines) and cumulative sequential heat (dashed lines) for three regional climate model (RCM) models in Hachioji, Japan. Historical data are represented in black and future RCM projections in gray. No change in cumulative sequential chill is projected; hence the historical and RCM lines coincide.

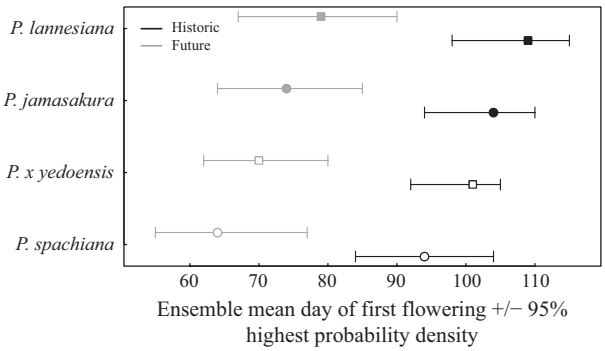

Fig. 7 Daily probability of first flowering for *P. spachiana*, *P.* × *yedoensis P. jamasakura*, and *P. lannesiana* for historical (1981–2000, black symbols) and future (2081–2100, gray symbols) periods based on the ensemble mean of three RCMs (NHRCM, NRAMS, and TWRF) downscaled to the Hachioji Meteorological Station. First flowering dates are forecast to shift 30–31 days earlier, with greater ranges of uncertainty, by 2100 under the A1B scenario.

Discussion

Our application of Bayesian survival regressions to first flowering events is novel in ecological, climate change, phenological, and horticultural literature. We expect plants to respond to temperatures on the scale of seconds to days and the accumulation approach allowed us to model these short-term responses. Unlike typical implementations of accumulation models, however, we are able to readily quantify uncertainty in our predictions. We are able to identify cases where more uncertainty exists prior to our first flowering date estimate than after, or *vice versa* (e.g., *P. jamasakura* in 1991, Fig. 5). We were also able to identify instances with multiple flowering probability peaks (e.g., *P.* × *yedoensis* in 1991, Fig. 5). Secondary daily flowering probability peaks corresponded to short-term warm spells that accelerated heat unit accumulation (Fig. 5; Figures S1, S3, S5, S7, S9).

Physiological processes that trigger flowering appear to occur in sequence for Japanese cherries. A sequential model is often used in models that include both chill and heat (Chuine, 2000; Linkosalo *et al.*, 2006) and corresponds with our understanding of plant physiology and phenology (Caffarra *et al.*, 2011). Temperate species with chilling requirements, like cherries, must experience some amount of chilling before warm springtime temperatures are effective for promoting breaking of dormancy (Sarvas, 1974; Arora *et al.*, 2003; Linkosalo *et al.*, 2006; Jimenez *et al.*, 2010). Models in the ecological literature that include temperature directly are

common (e.g., Menzel *et al*., 2006; Miller-Rushing *et al*., 2007; Primack *et al*., 2009), but including chill and heat here provided a more mechanistic understanding of Japanese cherry flowering phenology and avoided the potential statistical pitfall of the Modifiable Temporal Unit Problem (de Jong & de Bruin, 2012).

The 95% credible intervals of the chill parameter in our best fit model (Model 1) overlapped zero, yet this model still improved model fit over alternative candidate models. We found no strong pairwise correlations among our predictors which suggests that an underlying multivariate correlation structure in the data is driving the improved fit. Specifying a sequential model without chill is potentially spurious because the start of heat accumulation would still be defined by the satisfaction of chilling requirements (hence chill would still be indirectly in the model). However, the improved fit (5–18 DIC points) of the parallel cumulative heat + cumulative chill + microsite model (Model 6) over the parallel cumulative heat + microsite model (Model 5) suggests that chill is an important explanatory variable for this system (Fig. 2). Antagonistic genetic expression in some species, such that sufficient cold temperatures are needed to override photoperiod dormancy signals, also suggests that chilling and heating temperatures are biologically necessary in mechanistic models of temperate woody plant phenology (Jimenez *et al*., 2010). The inclusion of chill, which is receiving revitalized attention in the phenological literature (Caffarra *et al*., 2011; Polgar & Primack, 2011; Cook *et al*., 2012), was also critical to understanding years when plants were predicted to flower later than observed due to delayed fulfillment of chilling requirements (e.g., 1987, Fig. 5).

Our analysis highlights a few additional important points about modeling springtime flowering phenology. First, the choice of chill models does affect model performance. The UT model provided a much better model fit than the simpler, binary CH model (ΔDIC between Models 11 and 12 = 34.5, 20.9, 59.1, and 23.9 for *P. spachiana*, *P. jamasakura*, *P.* × *yedoensis*, and *P. lannesiana*), which is consistent with previous studies (Chuine, 2000; Alburquerque *et al*., 2008; Luedeling *et al*., 2009a). Second, microsite factors were less important predictors than weather, but still helped to explain the flowering phenology of these Japanese cherries. At this site, which has a small elevation range but steep slopes, lower elevation could result in cooler temperatures due to cold air drainage or other site-level factors. Our temperature loggers did capture some of the microsite variation, but the topographical position of each tree represented variation in soil or local biotic characteristics in addition to microclimate variation. Finally, sunlight hours did not significantly improve model fit (except for *P. lannesiana*, ΔDIC Models 8 and 9 = 17), but this measure of light may or may not have an effect similar to photoperiod. Sunlight hours are a measure of bright light and can vary on any given day from year to year unlike photoperiod. Essentially, sunlight hours are providing a proxy for solar radiation received (Suehrcke *et al*., 2013), high values of which may have promoted flowering. *Prunus* species have shown little to no influence of photoperiod on bud break (Heide, 2008), though photoperiod may be an important trigger for springtime phenological events in some species (Chuine *et al*., 2010; Basler & Körner, 2012).

The comparison of predictions from warmer and colder years and the high performance (based on DIC) of the sequential chill/heat model illustrates how important thresholds and chill/heat relationships can be. In our models, late predictions of first flowering dates typically occur in years with delayed fulfillment of chilling requirements. We set our chilling requirements based on available literature values for cherries (Alburquerque *et al*., 2008), but further physiological or experimental study could help refine the threshold and produce species-specific estimates. Fitting chilling requirements as a model parameter was not possible with our data due to non-identifiability that could be explored with future work, but the combinatorial nature of the fixed parameters here (e.g., accumulation start date, heat/chill relationship, chill requirement) suggests a model comparison approach may be more tractable (Terres *et al*., 2013).

The chill unit specifications we used are frequently used in horticultural studies of temperate woody species (Cesaraccio *et al*., 2004; Luedeling *et al*., 2009a,b) and the threshold values used to calculate chilling (Table 1) are critical to interpreting our results. The Utah chill (UT) algorithm was originally developed from physiological experiments relating air temperatures to plant dormancy in fruit trees (Richardson *et al*., 1974). The UT algorithm specifies that temperatures below 1.4 °C are too cold and above 9.1 °C are too hot for hormonal or enzymatic processes leading to flowering processes to occur (Anderson *et al*., 2001; Dirlewanger *et al*., 2012). The optimal temperature range for effective chilling (2.4–9.1 °C) then determines how chill accumulates and how quickly each plant reaches its chill requirement each year. For example, a very cold winter (e.g., temperatures below the lower bound of optimal chilling, 2.4 °C) followed by a cool spring could delay flowering because physiological processes are occurring slowly outside of their temperature optima. Alternatively, a warm winter followed by a warm spring could have a similar, but less dramatic delaying effect; chill requirements would be satisfied late, but rapid heat accumulation would promote

flowering quickly thereafter. Our study taxa do not show much variability in optimal temperatures for the simpler chill threshold model (Terres *et al.*, 2013) so we would not expect qualitatively different results using taxa-specific chill formulations in this analysis.

Forecast shifts in flowering phenology were driven more by projected accelerated heat accumulation than delays in meeting chill requirements. The projected temperature increases in winter and early spring still fall within the optimal chilling range of 2.4–9.1 °C in the Utah model, so we do not expect these cherries to change their response to early season temperatures. However, once the switch to heat accumulation occurs each year, heat units will accumulate faster due to higher temperatures and accelerate flowering time for all taxa. We expect that survival models that include sequential chill and heat to provide more realistic forecasts than heat-only models at sites where winter temperatures are projected to rise above the optimal 9.1 °C UT chilling threshold, causing slower chill accumulation as compared to historical rates. The consequence of slower chill accumulation remains unclear, but may include delayed flowering (Yua *et al.*, 2010) or erratic flowering.

Our projected flowering shift of about 1 month is similar to those for flowering cherries elsewhere. *Prunus* × *yedoensis* and *Prunus serrulata* were forecast to flower up to 4 weeks earlier by 2080 in the Mid-Atlantic region of the United States (Chung *et al.*, 2011) and *P. serrulata* 29 days earlier by 2100 in Korea (Chung *et al.*, 2009), both under the A2 emissions scenario. Dramatic shifts in timing have implications for the culturally and economically important cherry blossom festivals held throughout Japan and East Asia (Sakurai *et al.*, 2011). Festival organizers may have to shift the dates of these festivals substantially to retain the economic activity they generate, which accounts for about 40% of annual municipal revenue of some Japanese communities (Sakurai *et al.*, 2011). Some uncertainty in our forecasts shifts from after to before the mean flowering estimate under future climate, suggesting that perhaps timing the festivals to blooming will become slightly easier despite coming later. The socio-economic costs of temporal variation in cherry flowering extend to other regions as well; the cherry blossom festivals in the United States generate hundreds of millions of tourism dollars annually (National Cherry Blossom Festival, 2013) and agricultural cherry production is valued at nearly $1 billion in the United States alone (McKee, 2012).

Compared to regression models for the same data set (Miller-Rushing *et al.*, 2007), our models demonstrate mechanistically why February–March mean temperatures provided accurate predictions – these are the months when heating begins and continues to accumulate, once chilling requirements have been met. Such correspondence is not guaranteed in other systems or future climates, however, and the survival regression framework allows for a more direct assessment of driving mechanisms. Changes in plant phenology may also result in broader scale effects, such ecological mismatch (Pau *et al.*, 2011), degradation of ecosystem services (Burkle *et al.*, 2013), and shifts in carbon balance (Richardson *et al.*, 2009). Our mean forecasts of 30–31 days earlier first flowering of the cherries at the Tama Forest Garden, and our ability to explain such forecasts, is an important call to think critically about how and why organisms will respond to impending climate change so that we can untangle cascading effects as well.

Acknowledgements

Support for this collaborative project was provided by the US National Science Foundation (DEB 0842465) to J.A.S., R.B.P., and Inés Ibáñez. We thank Cory Merow, Inés Ibáñez, Robin Chazdon, and three anonymous reviewers for their critical feedback that improved this manuscript.

References

Alburquerque N, García-Montiel F, Carrillo A, Burgos L (2008) Chilling and heat requirements of sweet cherry cultivars and the relationship between altitude and the probability of satisfying the chill requirements. *Environmental and Experimental Botany*, **64**, 162–170.

Anderson JV, Chao WS, Horvath DP (2001) A current review on the regulation of dormancy in vegetative buds. *Weed Science*, **49**, 581–589.

Arora R, Rowland LJ, Tanino K (2003) Induction and release of bud dormancy in woody perennials: a science comes of age. *HortScience*, **38**, 911–921.

Basler D, Körner C (2012) Photoperiod sensitivity of bud burst in 14 temperate forest tree species. *Agricultural and Forest Meteorology*, **165**, 73–81.

Burkle LA, Marlin JC, Knight TM (2013) Plant-pollinator interactions over 120 years: loss of species, co-occurrence, and function. *Science*, **339**, 1611–5.

Caffarra A, Donnelly A, Chuine I, Jones MB (2011) Modelling the timing of *Betula pubescens* budburst. I. Temperature and photoperiod: a conceptual model. *Climate Research*, **46**, 147–157.

Cannell MGR, Smith RI (1984) Spring frost damage on young *Picea sitchensis* 2. Predicted dates of budburst and probability of frost damage. *Forestry*, **57**, 177–197.

Cannell MGR, Smith RI (1986) Climatic warming, spring budburst and frost damage on trees. *Journal of Applied Ecology*, **23**, 177–191.

Cesaraccio C, Spano D, Snyder RL, Duce P (2004) Chilling and forcing model to predict bud-burst of crop and forest species. *Agricultural and Forest Meteorology*, **126**, 1–13.

Chuine I (2000) A unified model of budburst in trees. *Journal of Theoretical Biology*, **207**, 337–347.

Chuine I, Morin X, Buggman H (2010) Warming, Photoperiods, and tree Phenology. *Science*, **329**, 277–278.

Chung U, Jung J-E, Seo H-C, Yun JI (2009) Using urban effect corrected temperature data and a tree phenology model to project geographical shift of cherry flowering date in South Korea. *Climatic Change*, **93**, 447–463.

Chung U, Mack L, Yun JI, Kim SH (2011) Predicting the timing of cherry blossoms in Washington, DC and Mid-Atlantic states in response to climate change. *PLoS ONE*, **6**, e27439.

Clark JS (2004) Why environmental scientists are becoming Bayesians. *Ecology Letters*, **8**, 2–14.

Cook BI, Wolkovich EM, Parmesan C (2012) Divergent responses to spring and winter warming drive community level flowering trends. *Proceedings of the National Academy of Sciences of the United States of America*, **109**, 9000–9005.

Cox DR (1972) Regression models and life tables. *Journal of Royal Statistical Society Series B (Methodological)*, **34**, 187–220.

Cox DR, Oakes D (1984) *Analysis of Survival Data*. CRC Press, New York.

Dasguptaa AS, Self G, Dadgupta S (2007) Non-identifiable parametric probability models and reparametrization. *Journal of Statistical Planning and Inference*, **137**, 3380–3393.

Dirlewanger E, Quero-García J, Le Dantec L *et al.* (2012) Comparison of the genetic determinism of two key phenological traits, flowering and maturity dates, in three *Prunus* species: peach, apricot, and sweet cherry. *Heredity*, **109**, 280–292.

Ellison AM (2004) Bayesian inference in ecology. *Ecology Letters*, **7**, 509–520.

Gelman A, Carlin JB, Stern HS, Rubin DB (2004) *Bayesian Data Analysis*. Chapman & Hall/CRC, Boca Raton.

Gienapp P, Hemerik L, Visser ME (2005) A new statistical tool to predict phenology under climate change scenarios. *Global Change Biology*, **11**, 600–606.

Gonzalez-Megıas A, Menendez R (2012) Climate change effects on above- and below-ground interactions in a dryland ecosystem. *Philosophical Transactions of the Royal Society B*, **367**, 3115–3124.

Hanninen H (1990) Modelling bud dormancy release in trees from cool and temperate regions. *Acta Forestalia Fennica*, **213**, 1–47.

Heide OM (2008) Interaction of photoperiod and temperature in the control of growth and dormancy of *Prunus* species. *Scientia Horticulturae*, **115**, 309–314.

Iizumi T, Semenov MA, Nishimori M, Ishigooka Y, Kuwagata T (2012) ELPIS-JP: a dataset of local-scale daily climate change scenarios for Japan. *Philosophical Transactions of the Royal Society – A*, **370**, 1121–1139.

Jimenez S, Reighard GL, Bielenberg DG (2010) Gene expression of DAM5 and DAM6 is suppressed by chilling temperatures and inversely correlated with bud break rate. *Plant Molecular Biology*, **73**, 157–167.

de Jong R, de Bruin S (2012) Linear trends in seasonal vegetation time series and the modifiable temporal unit problem. *Biogeosciences*, **9**, 71–77.

Kramer K (1994) Selecting a model to predict the onset of growth of *Fagus sylvatica*. *Journal of Applied Ecology*, **31**, 172–181.

Linkosalo T, Häkkinen R, Hänninen H (2006) Models of the spring phenology of boreal and temperate trees: is there something missing? *Tree Physiology*, **26**, 1165–1172.

Luedeling E, Zhang M, McGranahan G, Leslie C (2009a) Validation of winter chill models using historic records of walnut phenology. *Agricultural and Forest Meteorology*, **149**, 1854–1864.

Luedeling E, Zhang M, Luedeling V, Girvetz EH (2009b) Sensitivity of winter chill models for fruit and nut trees to climatic changes expected in California's Central Valley. *Agriculture, Ecosystems and Environment*, **133**, 23–31.

Martinussen T, Scheike TH (2006) *Dynamic Regression Models for Survival Data*. Springer, New York.

McKee G (2012) Cherries profile. Agricultural Marketing Center. Available at: http://www.agmrc.org/commodities__products/fruits/cherry-profile/ (accessed 19 April 2013).

Menzel A, Sparks T, Estrella N *et al.* (2006) European phenological response to climate change matches the warming pattern. *Global Change Biology*, **12**, 1969–1976.

Miller-Rushing A, Katsuki T, Primack R, Ishii Y, Lee SD, Higuchi H (2007) Impact of global warming on a group of related species and their hybrids: cherry tree (Rosaceae) flowering at Mt. Takao, Japan. *American Journal of Botany*, **94**, 1470–1478.

Miller-Rushing AJ, Inouye D, Primack RB (2008) How well do first flowering dates measure plant responses to climate change? The effects of population size and sampling frequency. *Journal of Ecology*, **96**, 1289–1296.

Nagata H, Yurugi Y (1982) Phenological studies in woody plants (II) flowering in cherry trees. *Bulletin of the Faculty of Agriculture Mie University*, **64**, 11–20.

National Cherry Blossom Festival (2013) Available at: http://www.nationalcherryblossomfestival.org/about/links/ (accessed 21 February 2013).

Nord EA, Lynch JP (2009) Plant phenology: a critical controller of soil nutrient resource acquisition. *Journal of Experimental Botany*, **60**, 1927–1937.

Parmesan C, Yohe G (2003) A globally coherent fingerprint of climate change impacts across natural systems. *Nature*, **421**, 37–42.

Pau S, Wolkovich EM, Cook BI *et al.* (2011) Predicting phenology by integrating ecology, evolution and climate science. *Global Change Biology*, **17**, 3633–3643.

Plummer M, Best N, Cowles K, Vines K (2006) CODA: convergence diagnosis and output analysis for MCMC. *R News*, **6**, 7–11.

van de Pol M, Cockburn A (2011) Identifying the critical climatic time window that affects trait expression. *The American Naturalist*, **177**, 698–707.

Polgar CA, Primack RB (2011) Leaf-out phenology of temperate woody plants: from trees to ecosystems. *New Phytologist*, **191**, 926–941.

Primack RB, Ibáñez I, Higuchi H, Lee SD, Miller-Rushing AJ, Wilson AM, Silander JA (2009) Spatial and interspecific variability in phenological responses to warming temperatures. *Biological Conservation*, **142**, 2569–2577.

R Core Team (2011) R: *A Language and Environment for Statistical Computing*. R Foundation for Statistical Computing, Vienna, Austria.

Richardson EA, Seeley SD, Walker DR (1974) A model for estimating the completion of rest for 'Redhaven' and 'Elberta' peach trees. *HortScience*, **9**, 331–332.

Richardson AD, Hollinger DY, Dail DB, Lee JT, Munger JW, O'Keefe J (2009) Influence of spring phenology on seasonal and annual carbon balance in two contrasting New England forests. *Tree Physiology*, **29**, 321–331.

Root TL, MacMynowski DP, Mastrandrea MD, Schneider SH (2005) Human-modified temperatures induce species changes: joint attribution. *Proceedings of the National Academy of Science of the United States of America*, **102**, 7465–7469.

Sakurai R, Jacobson SK, Kobori H, Primack R, Oka K, Komatsu N, Machida R (2011) Culture and climate change: Japanese cherry blossom festivals and stakeholders' knowledge and attitudes about global climate change. *Biological Conservation*, **144**, 654–658.

Sarvas R (1974) Investigations on the annual cycle of trees. II. Autumn dormancy and winter dormancy. *Communicationes Instituti Forestalis Fenniae*, **84**, 1–101.

Schaber J, Badeck F-W (2003) Physiology-based phenology models for forest tree species in Germany. *International Journal of Biometeorology*, **47**, 193–201.

Sherman R, Mullen R, Haomin L, Zhendong F, Yi W (2008) Spatial patterns of plant diversity and communities in Alpine ecosystems of the Hengduan Mountains, northwest Yunnan, China. *Journal of Plant Ecology*, **1**, 117–136.

Spiegelhalter DJ, Best NG, Carlin BP, van der Linde A (2002) Bayesian measures of model complexity and fit (with discussion). *Journal of the Royal Statistical Society: Series B*, **64**, 583–640.

Suehrcke H, Bowden RS, Hollands KGT (2013) Relationship between sunshine duration and solar radiation. *Solar Energy*, **92**, 160–171.

Terres MA, Gelfand AE, Allen JM, Silander JA (2013) Analyzing first flowering event data using survival models with space and time-varying covariates. *Environmetrics*, **24**, 317–331.

Thompson R, Clark RM (2006) Spatio-temporal modelling and assessment of within-species phenological variability using thermal time methods. *International Journal of Biometeorology*, **50**, 312–322.

Venables WN, Ripley BD (2002) *Modern Applied Statistics with S*. Springer, New York.. 512 pp.

Visser ME, Schaper SV, Holleman LJM, Dawson A, Sharp P, Gienapp P, Caro SP (2011) Genetic variation in cue sensitivity involved in avian timing of reproduction. *Functional Ecology*, **25**, 868–877.

Wilson AM, Latimer AM, Silander JA Jr, Gelfand AE, de Klerk H (2010) Hierarchical Bayesian model of wildfire in a Mediterranean biodiversity hotspot: Implications of weather variability and global circulation. *Ecological Modelling*, **22**, 106–112.

Yua H, Luedeling E, Xu J (2010) Winter and spring warming result in delayed spring phenology on the Tibetan Plateau. *Proceedings of the National Academy of Sciences*, **107**, 22151–22156.

Supporting Information

Additional Supporting Information may be found in the online version of this article:

Supplement S1. Predicted cumulative and daily probability of first flowering curves and best model residuals for 1980–2009 for all four cherry taxa.
Supplement S2. Model R code for daily phenology model.